Water entry and exit with large displacements by simplified models

T.I. Khabakhpasheva[1], **A.A. Korobkin**[1], **Kevin J. Maki**[2] **and Sopheak Seng**[3]

[1] School of Mathematics, University of East Anglia, Norwich, UK,
e-mail: t.khabakhpasheva@uea.ac.uk, a.korobkin@uea.ac.uk
[2] Department of Naval Architecture and Marine Engineering, University of Michigan Ann Arbor, MI, 48109 USA, e-mail: kjmaki@umich.edu
[3] Bureau Veritas, Marine & Offshore Division - Research Department, France,
e-mail: sopheak.seng@bureauveritas.com

The two-dimensional problem of a symmetric wedge entering water and exiting from it thereafter at a time-dependent speed is considered. The pressure distribution along the wetted part of the wedge and the total hydrodynamic force acting on the wedge are calculated by three simplified models: the Original Wagner Model (OWM) of water entry and the Linearized Model of water exit (LME), the Modified Logvinovich Model (MLM) of entry and exit, and Generalized Wagner Model (GWM) of entry and exit. Computational Fluid Dynamics (CFD) simulations are used to generate reference results for the development and elaboration of the water exit models with large displacements, and to match these models with the GWM of water entry. A custom solver (CFD1) built on the open-source finite-volume CFD library OpenFOAM was originally used to numerically solve the Navier-Stokes equations governing the air-water flow (see Piro and Maki (2013) for more details). To start with the exit model, one needs to ensure that the entry stage is well predicted by both CFD and simplified models. However, the hydrodynamic forces and the pressure distributions predicted by the GWM from Khabakhpasheva et al. (2014) and by the MLM from Korobkin (2004) were found to be rather different from those by the CFD during the entry stage. To examine why the predictions are so different, only vertical motions of the symmetric wedge with the deadrise angle of 45 degrees are considered in detail, and special attention is paid to the end of the entry stage, where the wedge speed is small.

The accuracy of the CFD results is confirmed by running each case of the wedge motions twice by the OpenFOAM solvers developed by Piro and Maki (2013) and by Seng et al. (2014) referred to as CFD2. It was found that both OpenFOAM solvers provide close results (see Figure 1) and, therefore, are reliable. The GWM force shown in this figure is without account for the gravity effects. The Figure 1 demonstrates that the gravity provides an important contribution to the force at the end of the entry stage.

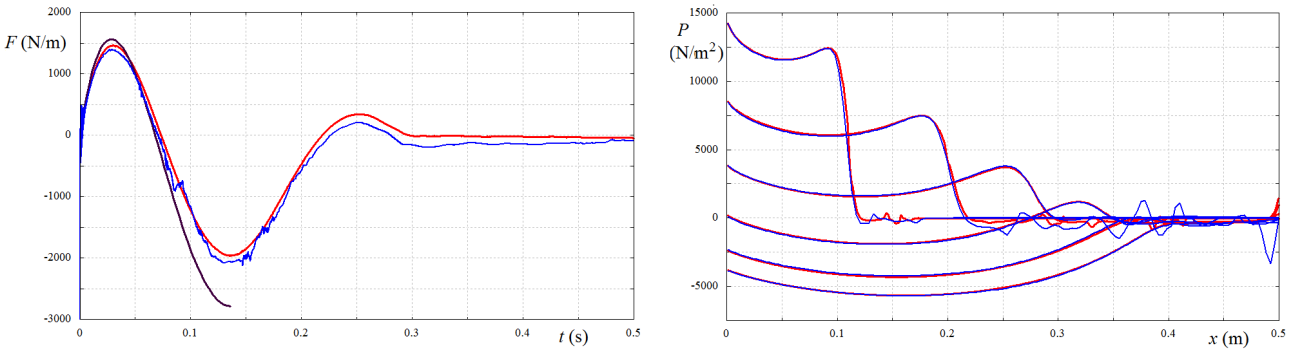

Fig. 1 The force and pressure distributions computed by CFD1 (red lines) and CFD2 (blue lines) together with the GWM force by numerical conformal mapping (black line) for case 2. Pressure profile at different instances of time [0.02, 0.04, 0.06, 0.08, 0.10, 0.12] s.

The numerical errors in GWM and MLM are minimized by using analytical formulae for the pressure distributions. The analysis of the obtained CFD and analytical results indicate the importance of gravity effects on the pressure distributions over the wetted part of the wedge. Gravity enters the solution through both the hydrostatic pressure and dynamic condition on the free surface. The prediction of the total hydrodynamic force by both GWM and MLM during the entry stage is improved when gravity effects are included. However, the pressure distributions predicted by the CFD and the simplified models are still rather different one from another. The pressure distribution predicted by the GWM is closer to the CFD prediction than that predicted by MLM. Calculations of the hydrodynamic forces are performed by the approach described in Korobkin et al. (2014), where the integration of the pressure along the wetted part of a body is performed only there where the component of the pressure proportional to the body speed squared is positive.

Conditions of computations

A rigid wedge with 45 degrees dead-rise angle enters the water, initially ($t < 0$) in $y < 0$, with a time-dependent speed. The position of the wedge is described by the equation $y = |x| - h(t)$, where $|x| < 0.5$ m, $h(t) = Vt - at^2/2$, V is the initial velocity of the wedge and a is a constant deceleration, $a > 0$. The gravitational acceleration is $g = 9.81$ m/s^2 and the water density is $\rho = 1000$ kg/m^3. No turbulence is included in the models. Four cases are simulated:

(1) $V = 2$ m/s, $a = g$ (without separation),
(2) $V = 4$ m/s, $a = 3g$ (without separation),
(3) $V = 4$ m/s, $a = 2g$ (with separation),
(4) $h(t) = h_0 \sin(At)$, $h_0 = 0.2$ m, $A = 10$ rad/s, $0 < t < 1$s .

Several quantities are studied to evaluate the model: the pressure distribution along the wedge wetted surface at several time instants, the pressure force as a function of time, the free surface elevation, and the pressure field. In the abstract we only report on the pressure force and pressure distribution on the wedge due to space limitations.

Water entry and exit by MLM

For the wedge of 45 degrees, the linearisation in MLM is performed at the level $y = kH(t)$, where $H(t)$ is the splash-up height, $H(t) = c(t) - h(t)$, and k is a parameter, $0 \le k \le 1$. Here $c(t)$ is the x-coordinate of the contact point in the Wagner model during the entry stage, $c(t) = \pi h(t)/2$, and in the linearised exit model (see Korobkin, 2013) during the exit stage. The factor k is taken as $1/2$ in the present calculations. The dynamic pressure distribution is given by

$$P_d(x,t) = -\rho\Big(\phi_t(x,t) + \frac{1}{2}\dot{h}(t)\phi_x + \frac{1}{4}\phi_x^2 - \frac{1}{4}\dot{h}^2(t)\Big),$$

where the velocity potential on the surface of the wedge, $\phi(x,t)$, is approximated by $\varphi^{(w)}(x,0,t) + \varphi_y^{(w)}(x,0,t)(|x| - h(t) - kH(t))$ during the entry stage, where $\varphi^{(w)}(x,y,t)$ is the velocity potential of the Wagner model of water impact, and by $\phi_t(x,t) = \varphi_t^{(e)}(x,0,t) + \varphi_{ty}^{(e)}(x,0,t)(|x| - h(t) - kH(t))$ during the exit stage, where $\varphi_t^{(e)}(x,y,t)$ is the acceleration potential of the linearised exit model from Korobkin (2013), $\varphi_t^{(e)}(x,0,t) = -\ddot{h}(t)\sqrt{c^2(t) - x^2}$ in the contact region. The derivative $\phi_x(x,t)$ is difficult to calculate at the exit stage. In the present calculations, the approximate formula $\phi_x(x,t) = x\dot{c}(t)/[c(t)\gamma]$ is used, where γ is a coefficient in the equation for $c(t)$, $\dot{c} = \gamma\varphi_x^{(e)}(c,0,t)$. The hydrostatic pressure is $P_s(x,t) = -\rho g[x - h(t)]$. The linearised dynamic boundary condition reads

$\varphi_t^{(e)} + g\eta(x,t) = 0$, where $y = \eta(x,t)$ is the elevation of the free surface, $|x| > c(t)$. The problems of water entry and exit with gravity are complicated, see Zekri et al. (2015). In our approach, $\eta(x,t)$ is approximated by $kH(t)$, which is the level of linearization in MLM. The correction to the pressure due to the gravity term in the dynamic condition is $P_c(x,t) = \rho g k[c-h]$. The total pressure $P_d + P_s + P_c$ is integrated along the wetted part of the wedge providing the total hydrodynamic force $F_{mlm}(t)$ acting on the wedge during its entry into water and subsequent exit from water. In the present calculations, $\gamma = 2\cos(\pi/4) = \sqrt{2}$, which accounts for the deadrise angle of the wedge. In calculations of the hydrodynamic force for bodies with small deadrise angle, $\gamma = 2$ was used, see Korobkin et al. (2014). The force by MLM is compared with the CFD force in Figure 2. Both $P_c(x,t)$ and $P_s(x,t)$ improve the theoretical prediction.

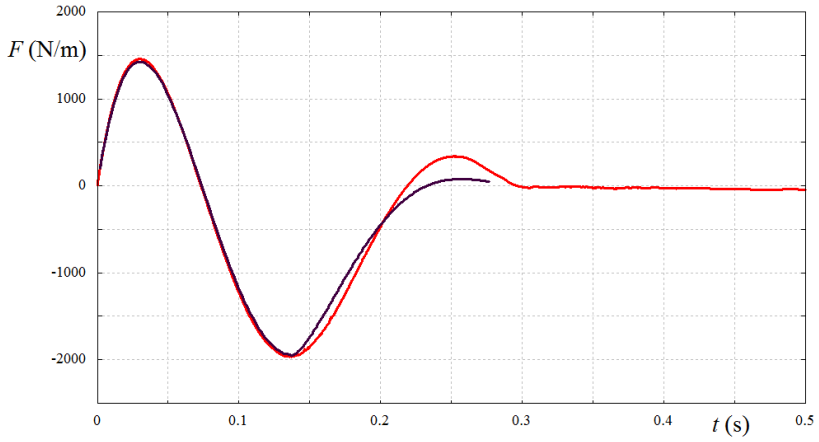

Fig. 2 The hydrodynamic force computed by CFD1 (red line) and by MLM (black line) for entry and exit stages for case 2.

Water entry and exit by GWM

The dynamic pressure $P_d(x,t)$ during the entry stage is given within the GWM in the parametric form, where $|\xi| < 1$ and γ is the wedge deadrise angle,

$$P_d(x, f(x) - h(t), t) = \rho\dot{h}^2(t)P_v(\xi) + \rho\ddot{h}(t)h(t)P_w(\xi),$$

$$P_v(\xi) = \frac{1}{2} - \frac{\tan\gamma}{N_0(\gamma)} + \frac{\sqrt{1-\xi^2}}{N_0(\gamma)\, w\cos\gamma} + \frac{q(\xi)}{N_0(\gamma)\, w\cos\gamma}\left(\frac{\xi}{\sqrt{1-\xi^2}}\right)^{1-2\gamma/\pi} - \frac{1}{2}\left(\frac{\xi}{\sqrt{1-\xi^2}}\right)^{2-4\gamma/\pi},$$

$$P_w(\xi) = \frac{1}{N_0(\gamma)\, w\cos\gamma}\Big[\sqrt{1-\xi^2} + \sin\gamma\,\big(q(\xi) - q(1)\big)\Big], \qquad x = \frac{q(\xi)h(t)}{N_0(\gamma)\, w},$$

$$q(\xi) = \int_0^{\xi}\left(\frac{\tau^2}{\tau^2-1}\right)^{\gamma/\pi} d\tau, \qquad w(\gamma) = q(1), \qquad c = \frac{h(t)}{N_0(\gamma)}, \qquad N_0(\gamma) = \frac{w(\gamma)\sin\gamma}{N_{00}(\gamma)},$$

$$N_{00}(\gamma) = \int_1^{\infty}\frac{\xi\, d\xi}{G^2(\xi)\sqrt{\xi^2-1}}, \qquad G(\xi) = 1 + \frac{1}{w\cos\gamma}\int_1^{\xi}\left(\frac{\tau^2}{\tau^2-1}\right)^{\gamma/\pi} d\tau.$$

The integrals in these formulae are evaluated with a controlled accuracy, in order to avoid any numerical errors. The total pressure distributions $P_d + P_s + P_c$, where the hydrostatic pressure P_s and the correction pressure P_c are the same as in MLM but with $k = 1$, which corresponds to

linearization of the free-surface boundary conditions at the splash-up height, are rather different from those by CFD. However, the total force by GWM with account for the gravity effects is very close to that by CFD, see Figure 3. The pressure distributions by MLM are also different from those by CFD, however, the total force by MLM is close to the force by CFD, see Figure 2.

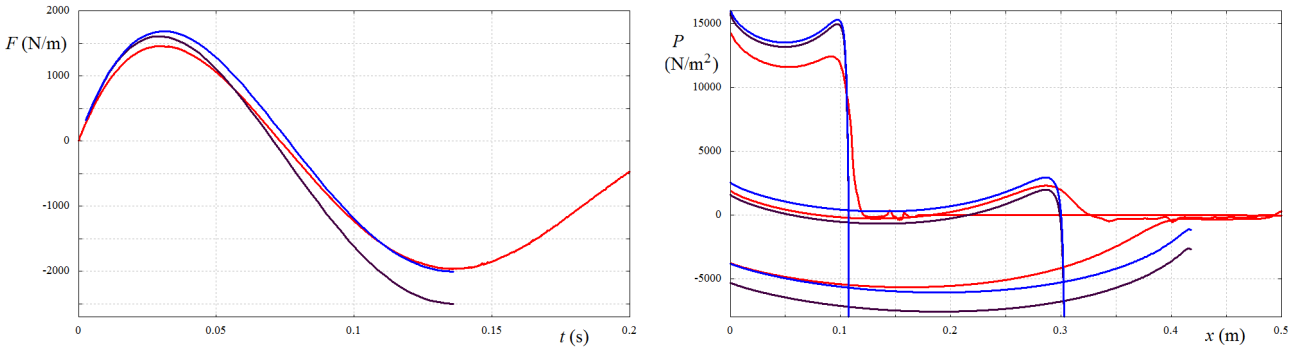

Fig. 3 The force and pressure distributions computed by CFD1 (red lines) and by GWM without the correction term P_c (black lines) and with this term (blue lines) for case 2. Pressure profile at different instances of time [0.02, 0.07, 0.12] s.

The hydrodynamic force during the exit stage is calculated by a new model which is based on the GWM ideas and the conformal mapping of the flow region onto a half-plane (Khabakhpasheva et al., 2014). However, during the exit stage, the problem is formulated with respect to the acceleration potential, $\varphi_t(x, y, t)$, as in the linearised exit model. The x-coordinate of the contact point is calculated by using the condition that the speed of this point is proportional to the local speed of the flow. This condition reads $\dot{c}(t) = \kappa \cos^2 \gamma \phi_x(c(t), t)$, where γ is the deadrise angle, κ is the coefficient of proportionality, and $\phi(x, t)$ was introduced in MLM section.

Acknowledgment: This work has been supported by the Office of Naval Research through the NICOP research grant "Fundamental Analysis of the Water Exit Problem" N62909-13-1-N274, administered by Dr. Woei-Min Lin, and the grants N00014-13-1-0558 and N00014-14-1-0577, administered by Kelly Cooper. Any opinions, findings, and conclusions or recommendations expressed in this material are those of the authors and do not necessarily reflect the views of the Office of Naval Research.

References

Khabakhpasheva, T. I., Kim, Y., & Korobkin, A. A. (2014). Generalised Wagner model of water impact by numerical conformal mapping. Applied Ocean Research, 44, 29-38.

Korobkin, A. (2004). Analytical models of water impact. Eur. Journal of Applied Mathematics, 15(06), 821-838.

Korobkin, A. A. (2013). A linearized model of water exit. Journal of Fluid Mechanics, 737, 368-386.

Korobkin A.A., Khabakhpasheva T.I., Maki K.J. (2014). Water-exit problem with prescribed motion of a symmetric body. Proc. 29th IWWWFB, , Osaka, Japan, p. 117-120.

Korobkin, A., Khabakhpasheva, T., Malenica, S., & Kim, Y. (2014). A comparison study of water impact and water exit models. International Journal of Naval Architecture and Ocean Engineering, 6(4), 1-1182.

Piro, D. J., Maki, K. J. (2013). Hydroelastic analysis of bodies that enter and exit water. Journal of Fluids and Structures, 37, 134-150.

Seng, S., Jensen, J. J., & Malenica, S. (2014). Global hydroelastic model for springing and whipping based on a free-surface CFD code (OpenFOAM). International Journal of Naval Architecture and Ocean Engineering, 6(4), 1024-1040.

Zekri, H. J., Korobkin, A. A., & Cooker, M. J. (2015) Liquid sloshing and impact in a closed container with high filling. Proc. 30th IWWWFB, , Bristol, UK.